applied sciences

MDPI

Article

Investigation of a Precise Control Scheme for Rice Quality

Yi Jin [1], Jun Yin [1], Huihuang Xie [2] and Zhongjie Zhang [1,*]

[1] National Engineering Research Centre for Grain Storage and Logistics, Academy of National Food and Strategic Reserves Administration, Beijing 100037, China; jy@ags.ac.cn (Y.J.); yjun@ags.ac.cn (J.Y.)
[2] Jiangsu Key Laboratory of Advanced Food Manufacturing Equipment and Technology, College of Mechanical Engineering, Jiangnan University, Wuxi 214122, China
* Correspondence: zzj@ags.ac.cn

Abstract: Rice drying is a complex and nonlinear process, with product quality being easily influenced by numerous factors. This study aimed to investigate the characteristics causing variation in rice quality and provide novel insights for regulating and controlling rice drying operations. To this end, response surface methodology was employed to examine the hot air drying of rice. The study was centered on investigating the impact of different levels of drying temperature (35–55 °C), relative humidity (30–50%), initial moisture content (20–28%), air velocity (0.36–0.84 m/s), and tempering ratio (1–4) on the process. The measured parameters included the net drying time, total drying time, additional crack percentage, and head rice yield. The experimental data were analyzed using Design–Expert, and the results indicated that all the response quadratic polynomial models were statistically significant. All the linear terms had a significant impact on the response variables except for the impact of air velocity on head rice yield. Finally, process reference charts of actual drying operating conditions were established based on the regression models to provide a scientific reference for guiding the control of rice drying quality and integrating into intelligent grain drying control systems in the future.

Keywords: rice; hot air drying; milling quality; quality control; process reference chart

check for updates

Citation: Jin, Y.; Yin, J.; Xie, H.; Zhang, Z. Investigation of a Precise Control Scheme for Rice Quality. *Appl. Sci.* **2023**, *13*, 7532. https://doi.org/10.3390/app13137532

Academic Editors: Daniel Cozzolino and Roberto Anedda

Received: 15 May 2023
Revised: 22 June 2023
Accepted: 23 June 2023
Published: 26 June 2023

Copyright: © 2023 by the authors. Licensee MDPI, Basel, Switzerland. This article is an open access article distributed under the terms and conditions of the Creative Commons Attribution (CC BY) license (https://creativecommons.org/licenses/by/4.0/).

1. Introduction

Rice, being one of the fundamental staple crops, ranks third in global production. Over half of the world's population relies on it as a dietary mainstay [1,2]. Due to seasonal and weather influences, the moisture content of rice harvested from fields often exceeds safe storage requirements, particularly in southern China where heavy rainfall is frequent. Rice with excess moisture will deteriorate due to infestation and mildew [3,4]. Therefore, it is imperative to conduct efficient drying treatment in order to ensure subsequent safe storage.

Grain drying is a complex and dynamic process involving mass and heat transfer. Currently, hot air drying is the predominant method used in industrial settings [5]. However, the moisture content of grains and various parameters of drying air (e.g., temperature, velocity, and relative humidity) are critical factors that can limit both efficiency and quality outcomes for operators [6]. If the operation relies solely on experience, improper treatment during the drying process may cause rice to crack. The kernel's tensile strength can be exceeded due to moisture and temperature gradients, inducing stress that leads to cracking. Cracked rice is typically the result of mechanical damage incurred during milling, which can negatively impact both on its taste and nutritional quality, ultimately leading to a decrease in economic value [7]. Therefore, it is imperative to ensure the quality of drying while reducing the moisture content of rice.

Several studies have been carried out to enhance the quality and efficiency of drying. Iguaz et al. [8] found that increases in temperature and air evaporation accelerated desiccation, resulting in an increase in cracked kernels and a decrease in head rice yield (HRY). Additionally, a moisture content reduction of more than 3% in a single drying step

could have negative effects on the overall kernel yield. Tohidi et al. [1] observed a similar relationship between drying rate and crack percentage while investigating the impact of air-drying parameters, such as temperature, velocity, and relative humidity, on rice during deep-bed drying. For grain drying, a tempering stage is often incorporated as a processing method, wherein the supply of hot air is halted after a period of drying to facilitate internal water equilibrium through heat and moisture gradients [9]. This leads to enhanced drying efficiency in the subsequent stage, resulting not only in reduced drying time and energy consumption but also guaranteed drying quality. Aquerreta et al. [10] discovered that tempering at 60 °C could significantly reduce drying time, decrease the incidence of cracking, and enhance HRY. Dong et al. [11] demonstrated that the internal water gradient and cracking of rice were significantly affected by both tempering temperature and duration. Compared to tempering at 20 °C, tempering at 50 °C resulted in a reduction in rice crack percentage ranging from 32% to 50%.

In addition to the aforementioned experimental findings, researchers have also endeavored to establish models for further regulating and optimizing grain drying. Shei and Chen [12] utilized a combined model of partial differential equation and two-step intermittent thin-layer drying equation for rough rice to simulate the drying characteristics of a dryer with intermittent circulation under various conditions, including different drying temperatures, absolute air humidities, drying times, and tempering durations. This study offers valuable insights for the operation and design of circulating grain dryers. Golmohammadi et al. [13] developed mathematical models to optimize the intermittent drying of rice in two stages by studying the drying and tempering processes. Different from a single empirical or theoretical model, Zecchi and Gerla [14] developed a drying–breakage model by integrating an empirical breakage model with a theoretical drying model, thereby enabling the prediction of drying time and the estimation of HRY. Nanvakenari et al. [15] investigated the impact of different fluidization regimes and temperatures in a fluidized bed dryer on rice drying time and quality characteristics. They developed an artificial neural network-based model using response surface methodology (RSM) to relate input and output variables. The RSM model outperformed the neural network in terms of prediction accuracy, enabling the optimization of the drying process based on this model.

Previous studies have offered guidance and recommendations for rice drying operations. However, it should be noted that an optimal process may not necessarily provide a high reference value due to the unique characteristics of rice drying when compared to fruit and vegetable drying. Variations in rice variety and water content at harvest can also result in significant differences in tempering ratios among grain dryers with varying structural designs [9,11]. Therefore, it is imperative to select a process plan based on the specific situation under consideration. In this study, a representative of the available thin-layer drying equipment was utilized for conducting hot air-drying experiments that mirrored actual drying processes. The effects of various parameters, such as drying temperature, relative humidity, initial moisture content, air velocity, and tempering ratio, were analyzed with respect to their impact on both milling quality and drying time. The experiments were designed using the Design–Expert v8.0.6.1 software (Stat-Ease Inc., Minneapolis, MI, USA) with RSM to investigate potential interactions among the parameters and construct regression models. Additionally, process reference diagrams were generated based on these models for drying time, ACP, and HRY. The novelty of these charts lies in their ability to demonstrate potential variations in grain quality throughout the drying process. By consulting these charts, users can ascertain the grain quality index at a specific time and location during drying without requiring actual quality testing. Additionally, presetting the quality index parameters enables obtaining corresponding operating parameters for the dryer, thereby providing guidance for effective grain drying operations and ensuring optimal drying outcomes. These charts can be utilized for predicting drying quality and searching for optimal processing conditions, thus providing a valuable resource for industrial-scale operations.

2. Materials and Methods

2.1. Sample Preparation

A freshly harvested high-quality early indica rice variety, MeiXiangZhan NO.2 (Guangdong, China), was selected for the experiments after screening to remove impurities and immature seeds. Prior to testing, the samples were naturally dried in a shaded and ventilated environment to reduce moisture content. A moisture analyzer (HS153, Mettler-Toledo, Zurich, Switzerland) was utilized for real-time measurement of the moisture content to ensure the experiments' required level was achieved. The samples were hermetically sealed in polyethylene bags and stored under refrigeration at an ambient temperature of 4 ± 1 °C and a relative humidity of $60 \pm 2.5\%$ prior to testing. Furthermore, the initial moisture content of the rice at harvest, as determined by drying for 24 h at 105 °C, was found to be 30% (wet basis, w.b.). The initial percentage of cracked grains was measured to be 1%, and natural drying had a negligible impact on this. The accuracy of the moisture analyzer had been calibrated using an oven method [16].

2.2. Drying Equipment and Procedure

The thin-layer drying experiments were conducted utilizing the system described by Jin [17], which could simulate a real-world drying environment. A schematic diagram of the experimental equipment is presented in Figure 1. The device enables the monitoring and control of temperature, relative humidity, and air flow rate during the drying process.

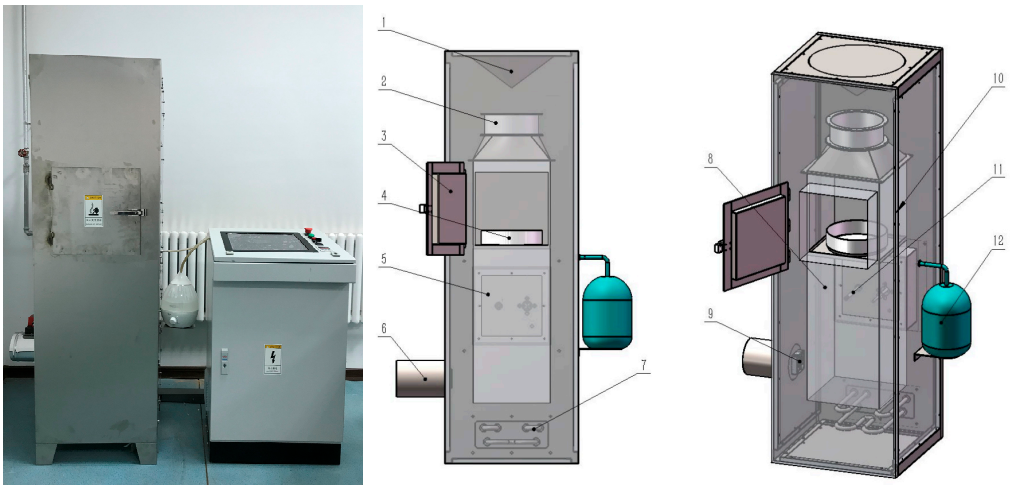

Figure 1. Multi-parameter hot-air thin-layer dryer: 1. wind shunt; 2. axial flow fan; 3. material bin door; 4. material tray; 5. sensor bin; 6. electric sealing valve; 7. heating pipe; 8. inner tank; 9. wet exhaust fan; 10. test-bed shell; 11. sensor group; and 12. humidifier.

In each experiment, the experimental parameters, such as drying temperature, air velocity, and relative humidity, were pre-set in the control panel of the dryer. The equipment was operated for at least 20 min to achieve steady-state conditions while the rice was removed from cold storage and placed in the environment. For each drying experiment, 1000 g of the rice sample was placed onto the material tray. A digital electronic scale (HZ3002B, China) with an accuracy of ± 0.01 g was utilized to record the weight of the rice every 15 min. The sample was then tempered in an oven at the same temperature and placed in a specially designed tempering box that had excellent sealing properties, thus effectively preventing moisture loss during tempering. All drying experiments were concluded when the moisture content reached 14% (w.b.).

2.3. Moisture Content

The moisture content (*MC*, w.b.) was calculated as follows:

$$MC = \frac{m_t - m_d}{m_t} \quad (1)$$

where m_t is the mass of the wet sample, and m_d is the mass of the dried sample.

2.4. Drying Time

The net drying time (Dtn) refers to the duration of the drying period in the dryer, excluding tempering time. On the other hand, the total drying time (Dtt) encompasses the entire length of time from the beginning to the end of the drying process.

2.5. Additional Crack Percentage

Rice cracking refers to the development of fissures in rice kernels. Because many scholars have observed these fissures occur after rapid drying [18,19], crack determination was uniformly conducted following sealed storage of the dried rice for 48 h. To determine the most accurate percentage of rice cracking, a sample of 300 grains was randomly selected and manually shelled before being placed on a lamp for observation. Then, a magnifying glass was used to meticulously document the quantity of cracked rice grains. The crack percentage (*Cp*) and additional crack percentage (*ACP*) were calculated, respectively, as follows:

$$Cp = \frac{n_c}{n_t} \times 100 \quad (2)$$

$$ACP = Cp_t - Cp_0 \quad (3)$$

where n_c and n_t represent the number of cracked grains and total grains, respectively, and Cp_t and Cp_0 represent the initial crack percentage and the crack percentage after drying, respectively.

2.6. Head Rice Yield

A 50 g sample of dried rice was subjected to two rounds of shelling using a laboratory-scale rice huller (JDMZ-100, China), followed by milling for 30 s to obtain head rice. The head rice was then separated from the broken rice using a rice appearance quality detector (JMWT-12, Beijing Oriental Fude Technology Development Co., LTD, Beijing, China), which required the input of both the brown rice ratio and the head rice ratio. The experiment was conducted three times and the average value was recorded as the result. The equation for the *HRY* is given as follows [20]:

$$HRY = \frac{B}{A} \times 100 \quad (4)$$

where *B* is the whole kernel weight (g), and *A* is the total weight of rice (g).

2.7. Experimental Design

The Design–Expert software was utilized to construct five-factor experiments via RSM. Optimal experimental designs were selected to reduce the number of trials and corresponding costs compared to a full factorial design. Additionally, fitting the results with a second-order model enabled the determination of interactions between the variables under investigation. A central composite design (CCD) was chosen as the experimental design for the RSM, comprising 59 experiment groups with 32 factorial designs, 10 axial points, and 17 central points. The primary experimental variables included drying temperature (T), relative humidity (RH), initial moisture content (MC), air velocity (V), and tempering ratio (TR). Their respective levels are detailed in Table 1. The levels of the factors were determined through a combination of empirical observation and extensive literature review.

It was assumed that the responses would be correlated with the independent variables via a second-order polynomial equation [21,22] as follows:

$$Y = \beta_0 + \sum_{i}^{5} \beta_i x_i + \sum_{i}^{5} \beta_{ii} x_{ii}^2 + \sum_{i \neq j=1}^{5} \beta_{ij} x_i x_j + \varepsilon \quad (5)$$

where Y is the response calculated by the model; β_0, β_i, β_{ii}, and β_{ij} are the regression coefficients for the intercept and the linear, quadratic, and interaction terms, respectively; and ε is the random error.

Table 1. Coded and uncoded values of five independent variables for the central composite design.

	Coded and Uncoded Values				
Factor	**$-\alpha$ = 2.378**	**−1**	**0**	**1**	**α = 2.378**
Drying temperature (T/°C)	35	40.8	45	49.2	55
Moisture content (MC/%)	20	22.3	24	25.7	28
Relative humidity (RH/%)	30	35.8	40	44.2	50
Air velocity (V/m/s)	0.36	0.5	0.6	0.7	0.84
Tempering ratio (TR)	1	1.9	2.5	3.1	4

Note: the tempering ratio is the ratio of tempering duration to the drying duration.

2.8. Process Reference Charts

According to the quadratic regression equation of the model, a combination of several indices was utilized to create process reference charts. Each chart plotted T (°C) on the horizontal axis and MC (%) on the vertical axis. Through extensive data collection from various industrial dryers, it was determined that air velocity typically ranged between 0.45 and 0.55 m/s, with a median value of 0.5 m/s selected as being optimal for these charts. To accommodate for the extreme conditions, relative humidities of 30%, 40%, and 50% were selected in the three cases, while tempering ratios were maintained at the moderate values of 2 and 3.

2.9. Statistical Analysis

The experimental data were analyzed using Design–Expert V8.0.6.1; this employed the analysis of variance (ANOVA), design matrix, regression analysis, correlation coefficients, and three-dimensional (3D) visualization plots. The statistical significance level for all tests was set at 0.05.

3. Results and Discussion

The experiments were conducted to investigate the effects of various parameters on rice and their interactions. The factor levels and corresponding response results for each experiment are listed in Table 2. The ANOVA results are presented in Tables 3 and 4, with a significant model and non-significant lack of fit at the 95% confidence level ($p > 0.05$). The polynomial models for each response, obtained from Equation (5), are presented in Table 5. The coefficient of determination (R^2) and the coefficient of variation (CV) were compared. CV is defined as the standard deviation expressed as a percentage of the mean value. A lower CV indicates higher data reliability, with values below 10% being desirable [23].

Table 2. Experimental data for various drying processes using the central composite design (CCD).

Runs	T (°C)	RH (%)	MC (%)	V (m/s)	TR	Dtn (min)	Dtt (min)	ACP (%)	HRY (%)
1	40.8	35.8	22.3	0.5	1.9	157.9	442.9	2.87	70.2
2	49.2	35.8	22.3	0.5	1.9	117.4	316.9	4.62	68.9
3	40.8	44.2	22.3	0.5	1.9	201.7	572.2	1.53	71.4
4	49.2	44.2	22.3	0.5	1.9	179.6	493.1	3.43	68.8
5	40.8	35.8	25.7	0.5	1.9	200.4	570.9	2.93	70.3
6	49.2	35.8	25.7	0.5	1.9	140	396.5	5.02	68.5
7	40.8	44.2	25.7	0.5	1.9	258.8	743.3	2.22	70.6
8	49.2	44.2	25.7	0.5	1.9	208.6	579.1	4.63	68.8
9	40.8	35.8	22.3	0.7	1.9	129.6	357.6	3.48	70.4
10	49.2	35.8	22.3	0.7	1.9	98.5	269.5	5.79	68.5
11	40.8	44.2	22.3	0.7	1.9	160.4	445.4	2.28	71.2
12	49.2	44.2	22.3	0.7	1.9	152.4	437.4	4.01	69.1
13	40.8	35.8	25.7	0.7	1.9	200.3	570.8	3.35	70.2
14	49.2	35.8	25.7	0.7	1.9	127.1	355.1	5.39	68.3
15	40.8	44.2	25.7	0.7	1.9	258.1	742.6	3.21	70.1
16	49.2	44.2	25.7	0.7	1.9	178.1	491.6	5.02	68.5
17	40.8	35.8	22.3	0.5	3.1	141.4	559.9	1.26	71.5
18	49.2	35.8	22.3	0.5	3.1	92.2	371.2	2.99	70.1
19	40.8	44.2	22.3	0.5	3.1	183.7	741.7	0.31	72.3
20	49.2	44.2	22.3	0.5	3.1	116.4	441.9	2.13	69.7
21	40.8	35.8	25.7	0.5	3.1	188.4	746.4	1.21	71.7
22	49.2	35.8	25.7	0.5	3.1	130	502	3.17	70.1
23	40.8	44.2	25.7	0.5	3.1	226.5	924	1	71.1
24	49.2	44.2	25.7	0.5	3.1	163	628	3.22	69.8
25	40.8	35.8	22.3	0.7	3.1	123.6	495.6	1.79	71.7
26	49.2	35.8	22.3	0.7	3.1	77.3	309.8	3.41	70.1
27	40.8	44.2	22.3	0.7	3.1	140	558.5	0.87	72
28	49.2	44.2	22.3	0.7	3.1	108.1	433.6	2.46	70.4
29	40.8	35.8	25.7	0.7	3.1	166.9	678.4	1.5	71.2
30	49.2	35.8	25.7	0.7	3.1	106.9	432.4	3.69	68.8
31	40.8	44.2	25.7	0.7	3.1	180	738	1.64	71.3
32	49.2	44.2	25.7	0.7	3.1	133.6	505.6	3.58	69.5
33	35	40	24	0.6	2.5	229.6	792.1	0.79	72.1
34	55	40	24	0.6	2.5	101.3	326.3	5.04	68.3
35	45	30	24	0.6	2.5	104.1	329.1	3.1	70.5
36	45	50	24	0.6	2.5	227	789.5	1.62	70.7
37	45	40	20	0.6	2.5	94	319	2.23	70.3
38	45	40	28	0.6	2.5	179.9	592.4	3.38	69
39	45	40	24	0.36	2.5	169.6	582.1	2.44	70.4
40	45	40	24	0.84	2.5	131.5	431.5	3.91	70.2
41	45	40	24	0.6	1	201.8	396.8	4.52	68.6
42	45	40	24	0.6	4	120	540	0.89	71.8
43	45	40	24	0.6	2.5	150	487.5	2.32	69.2
44	45	40	24	0.6	2.5	144.4	481.9	2.21	69.4
45	45	40	24	0.6	2.5	145.3	482.8	2.11	69.4
46	45	40	24	0.6	2.5	147.3	484.8	2.33	70
47	45	40	24	0.6	2.5	157.7	532.7	2.21	69.6
48	45	40	24	0.6	2.5	137.4	474.9	2.11	70.1
49	45	40	24	0.6	2.5	151.7	489.2	2.33	70.1
50	45	40	24	0.6	2.5	141.7	479.2	2.11	69.8
51	45	40	24	0.6	2.5	134.4	434.4	2.55	69.9
52	45	40	24	0.6	2.5	147.3	484.8	2.55	69.5
53	45	40	24	0.6	2.5	157.6	532.6	2.22	70.2
54	45	40	24	0.6	2.5	152.8	490.3	2.67	70
55	45	40	24	0.6	2.5	134.4	434.4	2.21	69.6
56	45	40	24	0.6	2.5	145	482.5	2.11	70.3
57	45	40	24	0.6	2.5	154.7	529.7	2.33	69.9
58	45	40	24	0.6	2.5	147.2	484.7	2.11	69.5
59	45	40	24	0.6	2.5	140.4	477.9	2.38	68.9

Table 3. Analysis of variance (ANOVA) results of drying time models.

Source	df	Drying Time (Net)		Drying Time (Total)	
		Sum of Squares	F-Value	Sum of Squares	F-Value
Model	20	87,941.38	51.87 **	1.02×10^6	40.17 **
T: Temperature	1	27,649.52	326.17 **	3.75×10^5	296.74 **
RH: Relative air humidity	1	20,578.66	242.76 **	2.36×10^5	186.31 **
MC: Moisture content	1	18,349.45	216.46 **	2.09×10^5	165.1 **
V: Air speed	1	4780.03	56.39 **	56,639.38	44.77 **
TR: Tempering ratio	1	10,810.37	127.52 **	60,791.82	48.05 **
T*RH	1	75.03	0.89	5.87	4.64×10^{-3}
T*MC	1	1205.41	14.22 **	16,366.93	12.94 **
T*V	1	36.13	0.43	1522.14	1.2
T*TR	1	105.85	1.25	15,819.76	12.51 **
RH*MC	1	57.78	0.68	308.14	0.24
RH*V	1	249.76	2.95	3467.36	2.74
RH*TR	1	1265.05	14.92 **	3804.1	3.01
MC*V	1	41.41	0.49	100.47	0.079
MC*TR	1	114.76	1.35	509.6	0.4
V*TR	1	62.16	0.73	3166.09	2.5
T^2	1	896.38	10.57 **	15,360.22	12.14 **
RH^2	1	904.88	10.67 **	15,395.35	12.17 **
MC^2	1	108.75	1.28	513.6	0.41
V^2	1	78.06	0.92	2471.69	1.95
TR^2	1	558.68	6.59 **	21.85	0.017
Residual	38	3221.3		48,072.37	
Lack of Fit	22	2373.58	2.04	36,175.52	2.21
Pure Error	16	847.72		11,896.86	
Cor Total	58	91,162.68		1.06×10^6	

Note: p-value < 0.01 is represented by **.

3.1. Drying Time

The drying time was divided into net drying time (Dtn) and total drying time (Dtt). Table 2 shows the different drying times under various conditions, with Dtn ranging from 77.3 to 258.8 min and Dtt ranging from 269.5 to 924 min. Due to tempering, there are significant variations in the Dtt values. According to the ANOVA results presented in Table 3, both Dtn and Dtt model F-values were found to be statistically significant at 51.87 and 40.17, respectively. Additionally, the lack-of-fit values are not significant, indicating that the model is indeed statistically significant. All factors demonstrate a significant impact on the rice sample's net drying time and total drying time ($p < 0.01$).

The F-value indicates the impact of a variable on the response, with a greater value indicating a stronger influence. Based on the F-value, the percentage contributions of each factor to Dtn and Dtt were determined (Figures 2a and 2b, respectively). The order of the factors affecting Dtn and Dtt was found to be consistent: T > RH > MC > TR > V. Therefore, air temperature, relative humidity, and moisture content are the primary influencing variables for controlling drying time. The impact of tempering on Dtt is less significant than that on Dtn, owing to the tempering effect. Taking into account the tempering stage, the duration of tempering increases proportionally with the ratio. However, it could accelerate the drying process to some extent and affect the overall trend of drying time variation.

Table 4. Analysis of variance (ANOVA) results of milling quality models.

Source	df	Drying Time (Net)		Drying Time (Total)	
		Sum of Squares	F-Value	Sum of Squares	F-Value
Model	20	84.52	123.79 **	56.09	25.05 **
T: Temperature	1	39.22	1148.95 **	33.93	303.1 **
RH: Relative air humidity	1	4.82	141.21 **	0.48	4.32 *
MC: Moisture content	1	2.44	71.54 **	2.59	23.14 **
V: Air speed	1	3.56	104.42 **	0.2	1.83
TR: Tempering ratio	1	26.98	790.24 **	14.56	130.03 **
T*RH	1	2.28×10^{-3}	0.067	0.07	0.63
T*MC	1	0.15	4.47 *	0.025	0.23
T*V	1	0.013	0.39	7.81×10^{-3}	0.07
T*TR	1	0.029	0.86	0.015	0.14
RH*MC	1	1.73	50.81 **	0.26	2.35
RH*V	1	2.28×10^{-3}	0.067	0.09	0.81
RH*TR	1	0.34	10.03 **	0.17	1.48
MC*V	1	0.029	0.86	0.38	3.42
MC*TR	1	2.81×10^{-5}	8.24×10^{-4}	0.038	0.34
V*TR	1	0.083	2.43	3.13×10^{-4}	2.79×10^{-3}
T^2	1	1.22	35.81 **	0.48	4.26
RH^2	1	0.1	2.99	1.58	14.11
MC^2	1	0.9	26.43 **	7.84×10^{-3}	0.07
V^2	1	2.17	63.63 **	0.69	6.19
TR^2	1	0.65	19.13 **	0.48	4.26
Residual	38	1.3		4.25	
Lack of Fit	22	0.82	1.24	1.9	0.59
Pure Error	16	0.48		2.36	
Cor Total	58	85.82		60.34	

Note: p-value < 0.01 is represented by **; p-value < 0.05 is represented by *.

Table 5. Second-order polynomial equation ignoring non-significant terms.

Response	Second-Order Polynomial Model Equation	R^2	CV (%)
Dtn	$Y = -319.54457 - 4.19846 \times T - 5.87506 \times RH + 51.29726 \times MC - 104.10679 \times V + 32.72127 \times TR - 0.86797 \times T*MC - 2.37116 \times RH*TR + 0.21134 \times T^2 + 0.21234 \times RH^2 + 7.41511 \times TR^2$	0.9545	6.03
Dtt	$Y = -1362.71399 - 3.21407 \times T - 52.57475 \times RH + 185.21498 \times MC - 358.36273 \times V + 436.73255 \times TR - 3.19833 \times T*MC - 8.38511 \times T*TR + 0.87549 \times T^2 + 0.87649 \times RH^2$	0.9399	7.05
ACP	$Y = 87.48851 - 0.71122 \times T - 0.96706 \times RH - 3.62912 \times MC - 18.85010 \times V - 4.08123 \times TR + 9.76691 \times 10^{-3} \times T*MC + 0.032925 \times RH*MC + 0.039009 \times RH*TR + 7.81273 \times 10^{-3} \times T^2 + 0.041955 \times RH^2 + 18.07766 \times V^2 + 0.25390 \times TR^2$	0.9818	6.76
HRY	$Y = 108.88074 - 0.64910 \times T - 0.68473 \times RH - 0.14540 \times MC - 12.91655 \times V - 0.16367 \times TR + 4.87314 \times 10^{-3} \times T^2 + 8.87314 \times 10^{-3} \times RH^2 + 10.19643 \times V^2 + 0.21658 \times TR^2$	0.9118	0.47

For a significance level of 0.05, the interaction terms T*MC and RH*TR, as well as the quadratic terms T^2, RH^2, and TR^2, exhibit significant effects on Dtn; for Dtt, significant effects were observed for T*MC, T*TR, T^2, and RH^2. To enhance the descriptive power of the model and ensure its simplicity and reliability, insignificant interaction and quadratic terms ($p > 0.05$) were eliminated to derive a regression equation for each response variable, and the results are presented in Table 5. The Dtn and Dtt regression models demonstrate a remarkably good agreement between the predicted and measured results, with corresponding R^2 values of 0.9545 and 0.9399, respectively. Additionally, the high reproducibility of these models is evidenced by their low CV values (CV < 10%) [24]. The ANOVA results indicate a strong agreement between the fitted models and experimental data for the regression equation.

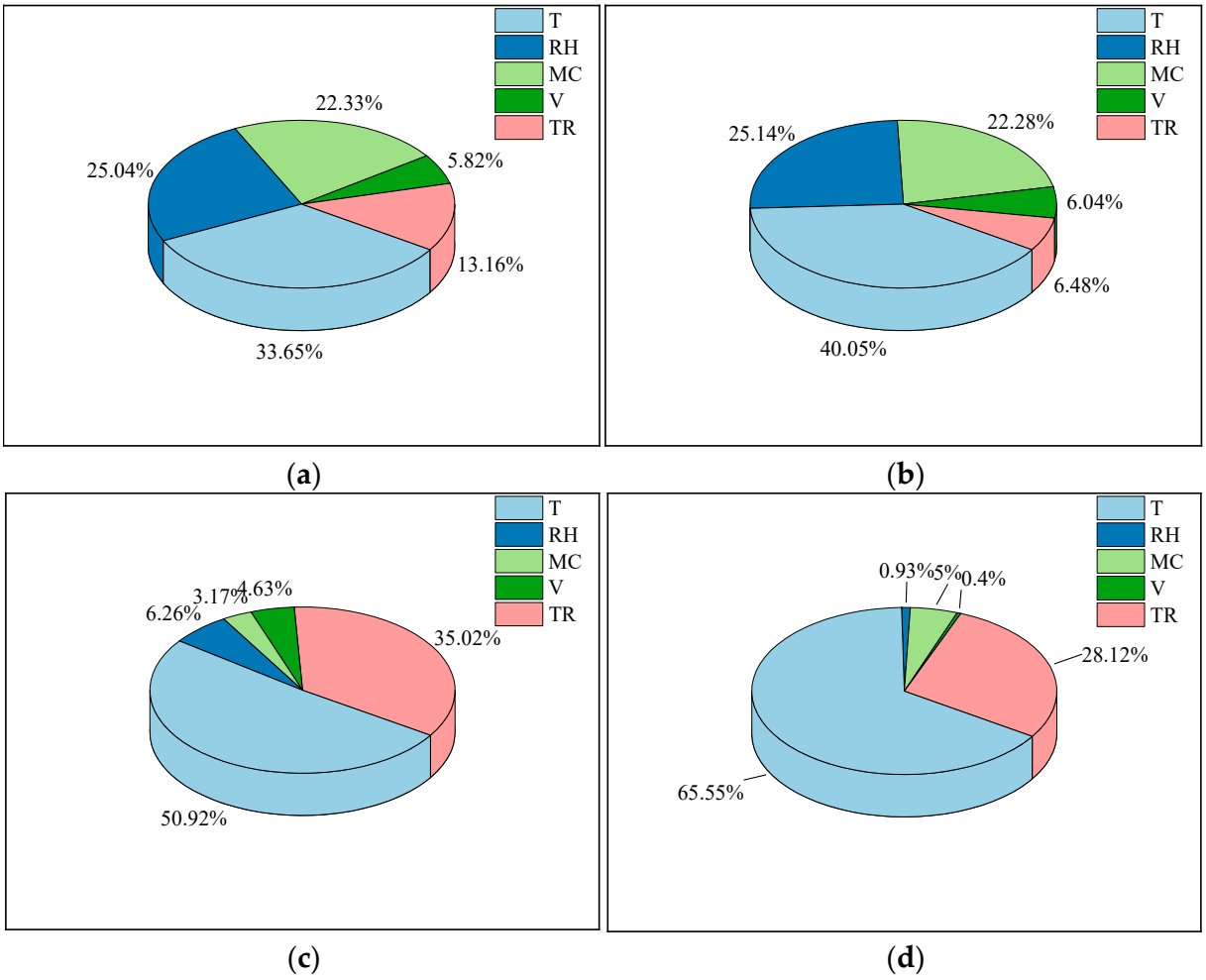

Figure 2. Percentage contributions of individual factors on (**a**) net drying time (Dtn), (**b**) total drying time (Dtt), (**c**) additional crack percentage (ACP), and (**d**) head rice yield (HRY).

Based on the significant interaction terms identified in the ANOVA results, a subset of factors was chosen for further analysis. Utilizing the Design–Expert software, 3D response surfaces and corresponding contours were generated (Figures 3–6). Factors that remained constant throughout the experimentation were set at a level of zero.

Increasing the drying temperature was found to be the most effective method of shortening the net drying time, as demonstrated in Figures 3 and 4. Additionally, Dtn values are superior with lower moisture contents and relative humidities, as well as higher tempering ratios. Notably, varying the moisture content and temperature within the low-drying-time region (lower right corner) does not significantly reduce the Dtn values compared to the high-drying-time region (upper left corner), as shown in Figure 3b. Excessive shortening of the Dtn through process adjustments does not result in significant benefits; rather, it could lead to considerable energy consumption, quality degradation, and other issues. Therefore, it is necessary to comprehensively consider these factors [25–27].

From Figure 4b, it can be observed that increasing the tempering ratio does not enhance the drying process significantly, particularly at low relative humidities. This implies that there exists a critical value of tempering duration beyond which prolongation would not lead to an improvement in drying efficiency. This could be attributed to the equilibrium of internal moisture during prolonged tempering, resulting in no further improvement in the net drying time.

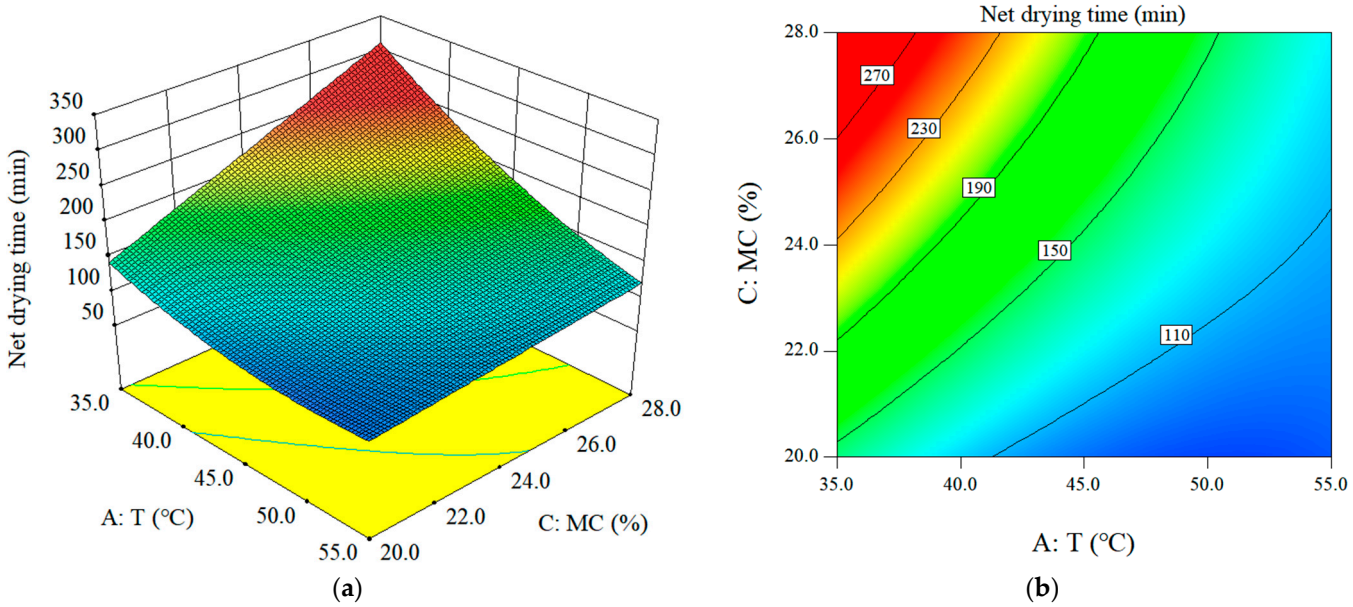

Figure 3. Interaction effects of MC and T on Dtn: (**a**) 3D surface and (**b**) contour.

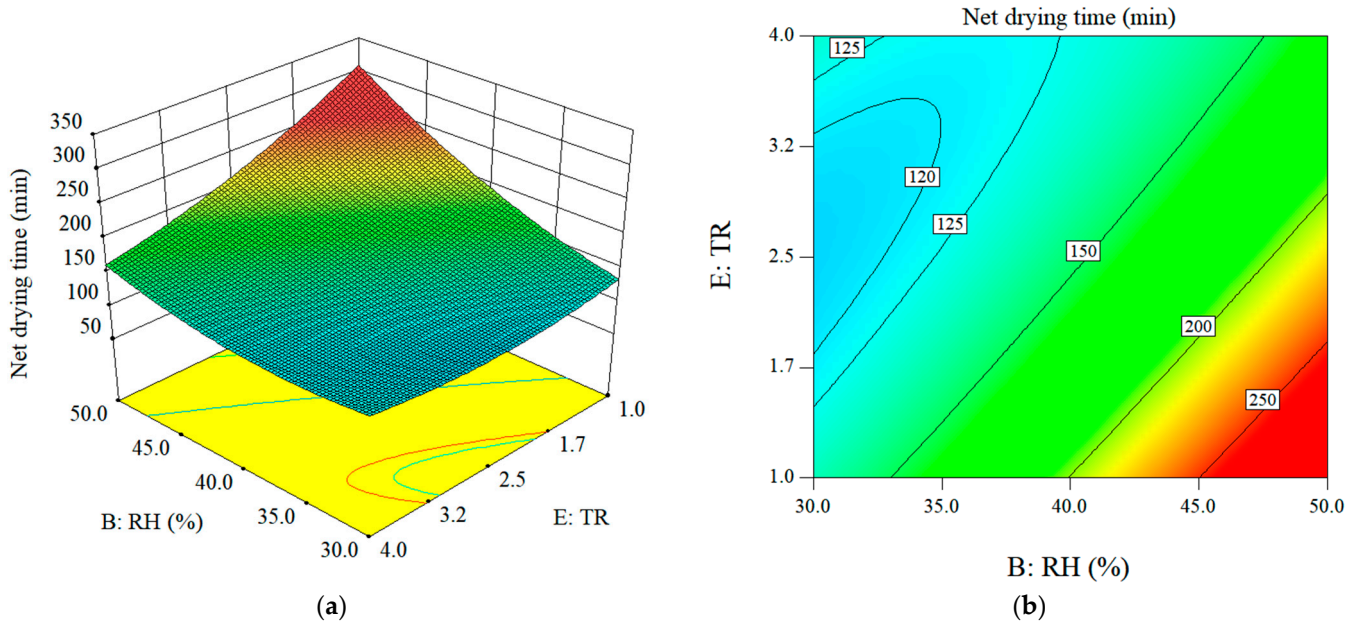

Figure 4. Interaction effects of RH and TR on Dtn: (**a**) 3D surface and (**b**) contour.

For the total drying time (as shown in Figures 5 and 6), the impact of drying temperature change was found to be most significant. The tempering ratio exhibits a direct proportionality with respect to the total drying time, unlike its effect on Dtn. In other words, under identical drying conditions, prolonging tempering would lead to an increase in both total drying time and rate of drying stage; this would subsequently enhance energy efficiency by discontinuing the hot air supply. In a study conducted by Bertotto et al. [28], it was discovered that a shorter tempering duration of 40–120 min could lead to reduced total drying time. However, this resulted in a slower rate during the drying stage and poor energy efficiency.

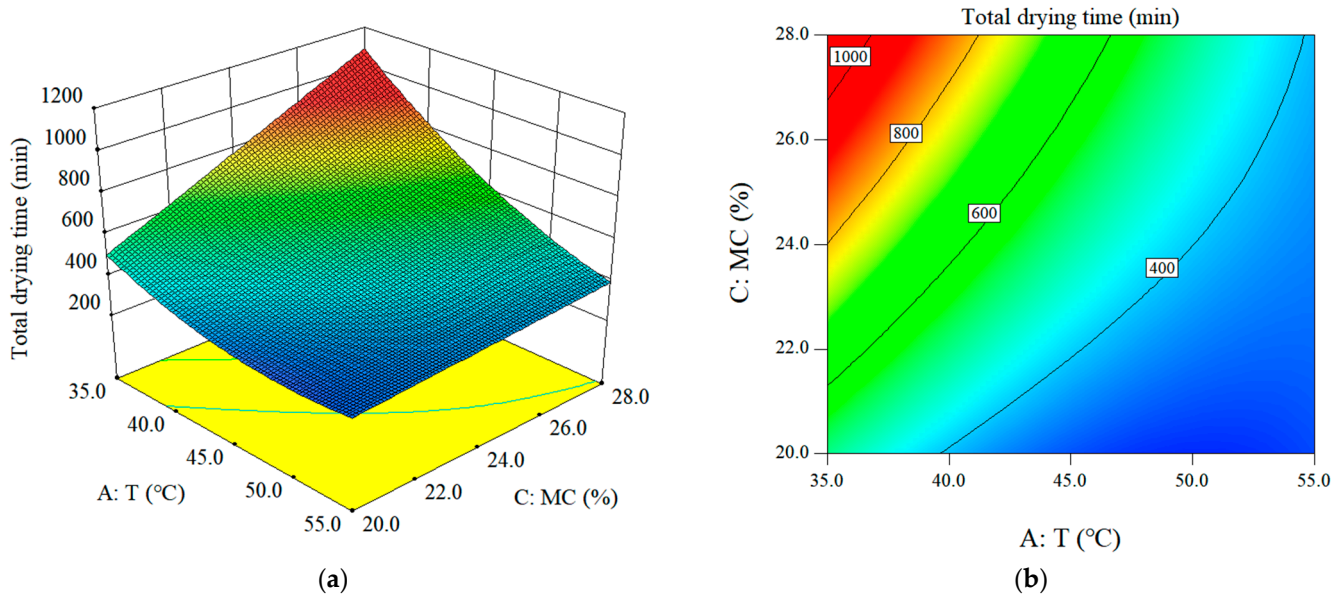

(**a**) (**b**)

Figure 5. Interaction effects of T and MC on Dtt: (**a**) 3D surface and (**b**) contour.

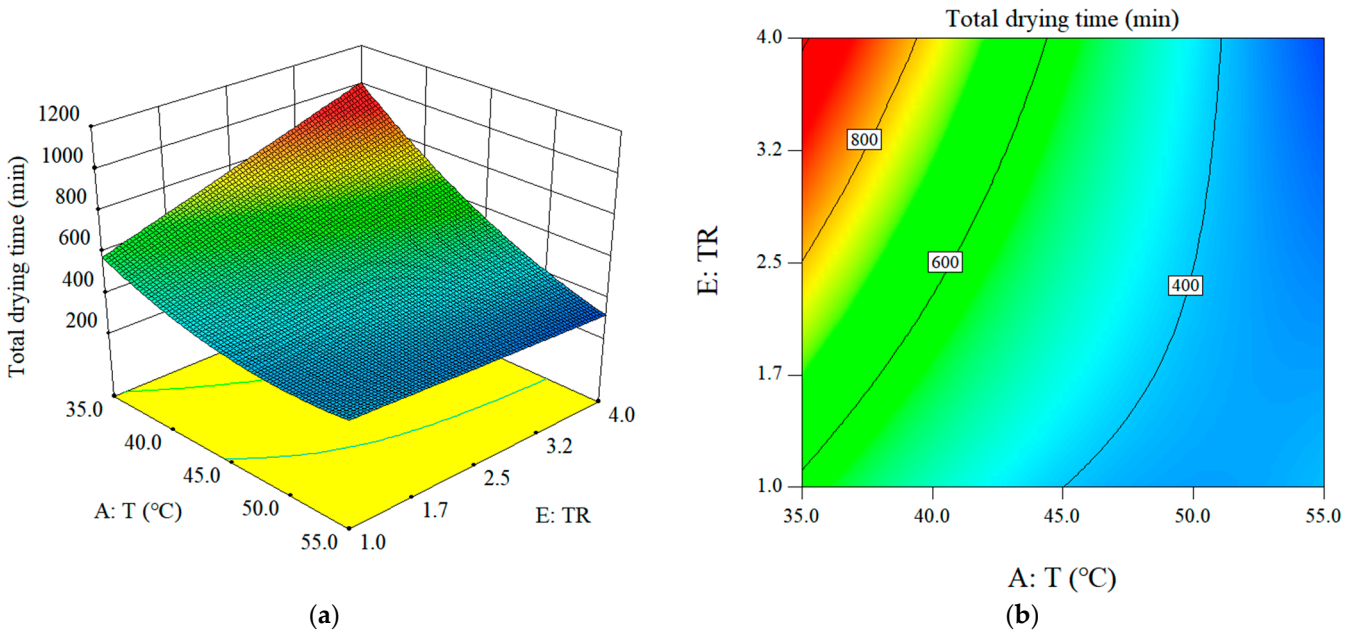

(**a**) (**b**)

Figure 6. Interaction effects of T and TR on Dtt: (**a**) 3D surface and (**b**) contour.

3.2. Milling Quality

3.2.1. Additional Crack Percentage

Rice cracking is a crucial indicator for assessing the quality of rice drying. Figure 7 illustrates the varying degrees of fissures present in rice kernels. The formation of cracks during the drying process was determined based on the ACP, with values ranging from 0.31% to 5.79%. Specific figures can be found in Table 2. All five factors demonstrate highly significant model terms ($p < 0.01$), as presented in Table 4. The ACP analysis depicts that the drying temperature and tempering ratio are the primary contributors, accounting for 50.92% and 35.02% in the variance, respectively, as illustrated in Figure 2c. At a significance level of $p < 0.05$, the interaction terms T*MC, RH*MC, and RH*TR, as well as the quadratic terms T^2, MC^2, V^2, and RT^2 were found to be statistically significant. The ACP regression equations were derived by eliminating non-significant interactions and quadratic terms

(see Table 3). With an R^2 value of 0.9819 and a CV value of 6.76, the model demonstrates excellent fitting ability and reliability.

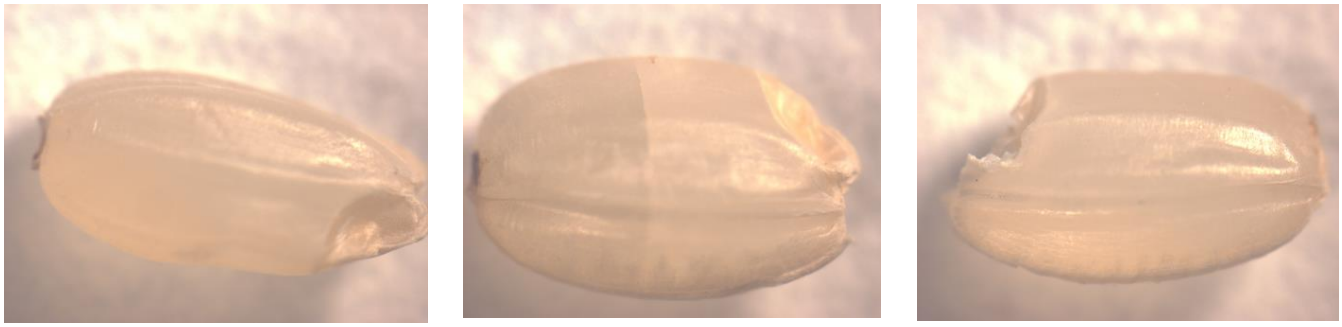

(**a**) (**b**) (**c**)

Figure 7. Comparison of different types of dried rice kernel (after hulling): (**a**) a whole rice kernel, (**b**) a rice kernel exhibiting a distinct fissure, and (**c**) a partially formed rice grain.

To investigate the interaction between the factors, response surfaces and contour plots were generated. Figures 8–10 depict four terms (T, RH, MC, and TR) that exhibit significant interaction effects on ACP. As illustrated in Figure 8a, an increase in drying temperature and initial moisture content results in a notable enhancement in ACP. As depicted in Figure 8b, the contour density along the drying temperature (T) direction exceeds that of the initial moisture content (MC) direction. This phenomenon suggests that an increase in ACP is more responsive to drying temperature, which is consistent with the previous F-value results. Within the temperatures' range of 47 °C to 55 °C, the contour lines become denser and the ACP changes dramatically. At higher temperatures, the ACP was found to be more sensitive to temperature. As depicted in Figure 8a, the ACP exhibits a positive correlation with relative humidity when the initial MC values are high (MC $\geq$ 26% w.b.), whereas at lower MC levels (<26%), an increase in relative humidity leads to a decrease in ACP, particularly at low initial moisture content levels. This observation is also supported by the density of the contour lines shown in Figure 9b. The ACP exhibits a minimum value at 50% relative humidity and an initial moisture content of 20%. As depicted in Figure 10, the larger the tempering ratio and relative humidity, the smaller the ACP becomes. However, at low levels of tempering ratio, the impact of relative humidity on the results is insignificant.

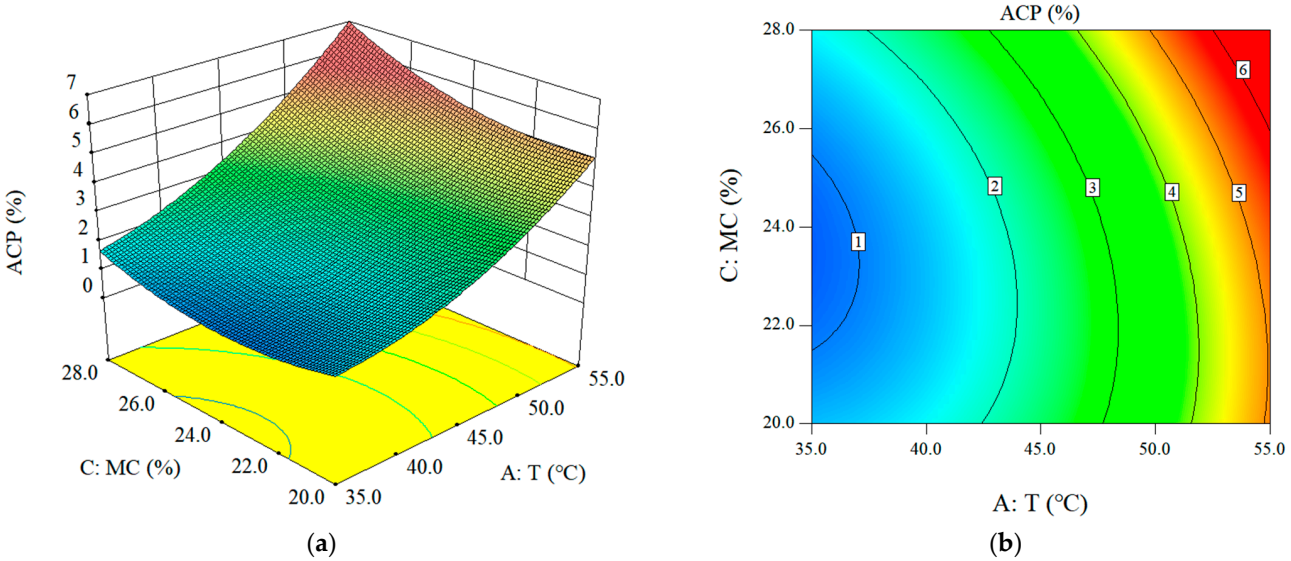

(**a**) (**b**)

Figure 8. Interaction effects of MC and T on ACP: (**a**) 3D surface and (**b**) contour.

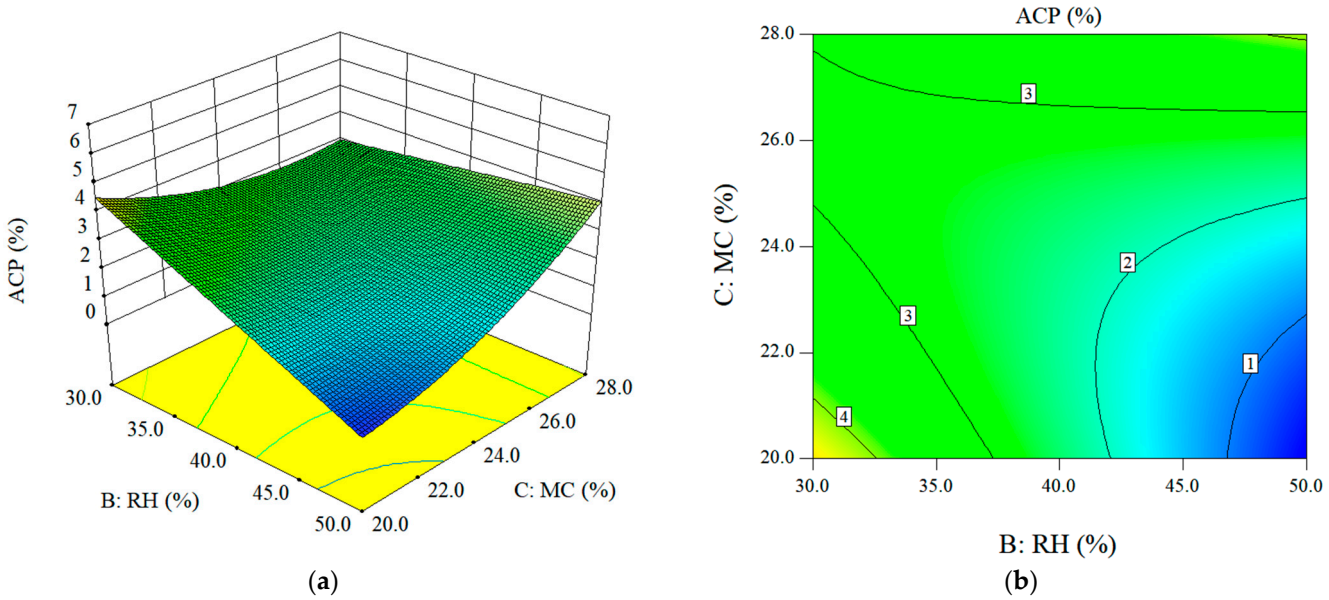

Figure 9. Interaction effects of RH and MC on ACP: (**a**) 3D surface and (**b**) contour.

3.2.2. Head Rice Yield

The head rice yield (HRY) serves as a direct indicator of the quality of milled rice, thus playing a crucial role in both rice grading and evaluation of drying quality. As shown in Table 2, the HRY values range from 68.3% to 72.3% across different processing methods. According to the ANOVA results presented in Table 4, all experimental factors exhibit significant influences on the HRY with the exception of air velocity (V). Figure 2d illustrates that drying temperature is the dominant factor affecting the HRY, followed by tempering ratio. At a significant level of $p < 0.05$, no interaction terms were found to be significant, while the quadratic terms T^2, RH^2, V^2, and TR^2 have notable effects. The HRY regression equation was derived by eliminating non-significant interactions and quadratic terms (Table 3). The R^2 value of the regression model is 0.9118, with a CV value of 0.47, indicating that the model exhibits excellent fitting ability and reliability.

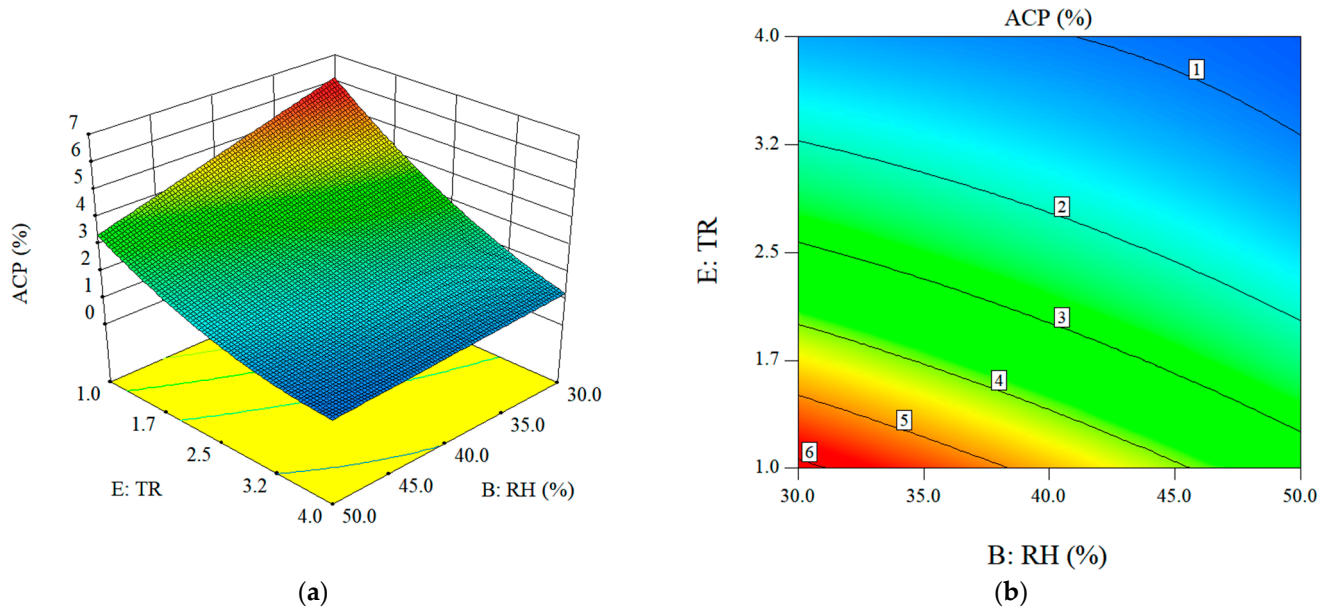

Figure 10. Interaction effects of TR and RH on ACP: (**a**) 3D surface and (**b**) contour.

3.3. Model Validation

To validate the established regression model, four sets of process parameter values were randomly generated within their respective ranges to conduct verification experiments. The predicted values were obtained through the regression equations, and the relative errors between the experimental and predicted values were calculated. As shown in Tables 6 and 7, most group errors fall within an acceptable range of 10% for engineering practice. This demonstrates the models' effectiveness in predicting various indicators.

Table 6. Predicted and measured values of drying time.

Run	Parametric Setting					Net Drying Time (min)			Total Drying Time (min)		
	T (°C)	RH (%)	MC (%)	V (m/s)	TR	Predicted	Measured	Discrepancy	Predicted	Measured	Discrepancy
1	37	45	27	0.7	2.4	283.7	301.4	6.23%	965.3	938.4	2.87%
2	52	45	23	0.8	1.5	172.5	168.5	−2.30%	465.8	480.1	2.98%
3	42	35	27	0.75	2	190.2	210.3	10.57%	562.2	545.3	3.1%
4	44	48	22	0.6	1.3	234.6	220.9	−5.84%	571.6	560.8	1.92%

Table 7. Predicted and measured values of milling quality.

Run	Parametric Setting					Net Drying Time (min)			Total Drying Time (min)		
	T (°C)	RH (%)	MC (%)	V (m/s)	TR	Predicted	Measured	Discrepancy	Predicted	Measured	Discrepancy
1	37	45	27	0.7	2.4	2.29	2.67	16.50%	71.57	71.2	−0.52%
2	52	45	23	0.8	1.5	6.4	6	−6.25%	68.54	68.1	−0.64%
3	42	35	27	0.75	2	3.94	4.33	9.90%	69.78	71.2	2.03%
4	44	48	22	0.6	1.3	2.45	2.5	2.04%	70.21	69.1	−1.58%

3.4. Process Reference Chart for Quality

The desirability function approach is a commonly employed technique in response surface methodology (RSM) for optimizing each response variable and determining the optimal drying conditions [29]. However, the process of drying grains differs from that of fruits and vegetables, and there is no fixed optimal drying method. The initial moisture content of rice is greatly influenced by factors such as harvest season, region, and variety. Due to the diversity of rice dryers and their varying structural types, tempering ratios may differ and operating environmental air humidity can fluctuate, thus necessitating real-time adjustments to dryer parameters [30]. In order to mitigate the impact of sensitive factors on drying quality and achieve precise control, for early indica rice with minimal varietal differences, process reference charts have been developed. This expedites the drying process while ensuring milling quality. These charts depict the projected values of one or multiple rice indices during drying under varying conditions. Additionally, the corresponding parameters of the drying process can be extracted from the charts to establish target values for one or more indices. Based on the experimental results and considering the sensitivity to factors and factor adjustability, the drying temperature was identified as the primary query process parameter in the process reference charts for different initial moisture contents and relative humidities. Figures 11 and 12 depict the process reference charts for tempering ratios of two and three, respectively, that are applicable to dryers with varying tempering ratios. These charts can be utilized for other grain types, such as corn or different varieties of rice, and integrated into intelligent drying control systems in the future.

The contours of the net drying time and ACP are presented in Figure 11, where the top left region exhibits longer net drying times and smaller ACPs. As the initial moisture content decreases and drying temperature increases, a decrease in net drying time is observed alongside an increase in ACP. Furthermore, under the influence of initial moisture content and drying temperature, opposite responses are noted for both drying time and ACP with varying trends. For a given ACP, the contour lines of varying relative humidities converge at a singular point. Above this point, the relative humidity exhibits a positive correlation with the ACP, while below this point, it shows a negative correlation. This further elucidates the interplay between RH and MC. To simultaneously satisfy both indicators' requirements, we divided the process area and established preferred zones

where desired responses could be achieved. According to the National Standards of the People's Republic of China, the ACP should not exceed 3%. For the net drying time, a moderate value of 200 min was selected based on the experimental results. The preferred area is where ACP $\leq$ 3% and DT $\leq$ 200 min achieve a suitable tradeoff at a specific relative humidity level. Figure 10a illustrates that the preferred area is enclosed by the DT at 40% RH, the ACP at 40% RH, and the *X*-axis and *Y*-axis at 40% RH. Assuming an initial moisture content of 24%, a chart search indicates that drying temperatures ranging from 40.9 °C to 45.3 °C are suitable options for the drying process design. However, in some exceptional cases, it may not be possible to establish the preferred areas to obtain this information. As depicted in Figure 11a, achieving a net drying time of less than 200 min at 50% relative humidity proves to be challenging. Under such circumstances, extending the drying duration is necessary to ensure optimal drying quality. Additionally, providing guidance for rice with an extremely high or low moisture content within the most favorable range presents difficulties. For high-moisture rice, we can reduce the moisture content to meet technological requirements through natural drying based on the reference chart in order to ensure compliance with the quality standards. However, when dealing with rice with an extremely low moisture content, adjusting the moisture level is not feasible and may lead to exceeding the ACP limits during drying. Fortunately, early indica rice varieties are widely cultivated in southern China and typically have higher levels of moisture.

In addition to being correlated with the drying time and quality indices, milling indices can also be correlated with multiple simultaneously selected quality indices. Figure 12 illustrates the reference process charts for both ACP and HRY. Unlike the trend of ACP, the HRY exhibits higher values in the region near the bottom left on both charts. The contour lines of the HRY are consistently linear within the parameter ranges due to the insignificant interactions between the factors, resulting in each factor independently affecting the HRY. As rice is often graded based on its HRY level, it becomes necessary to limit the value of HRY. Based on China's national standards for high-quality early indica rice, the first-grade, high-quality early indica rice standard was combined with the experimental data to establish a limit of HRY greater than 70%. The preferred high-quality area was divided in the same manner as shown in Figure 10 (ACP $\leq$ 3% and HRY $\geq$ 70%). The preferred regions vary under different relative humidity conditions. As shown in Figure 11a, when the relative humidity is at 30%, all areas where ACP $\leq$ 3% are within the range of HRY $\geq$ 70%. This suggests that the ACP serves as the primary control index under low relative humidity levels. With an RH below 40%, the coupling area is nearly identical to the region where the HRY exceeds 70%, and the process adjustments primarily focus on the HRY. Similar outcomes are observed in the HRY–ACP process reference chart with a tempering ratio of three.

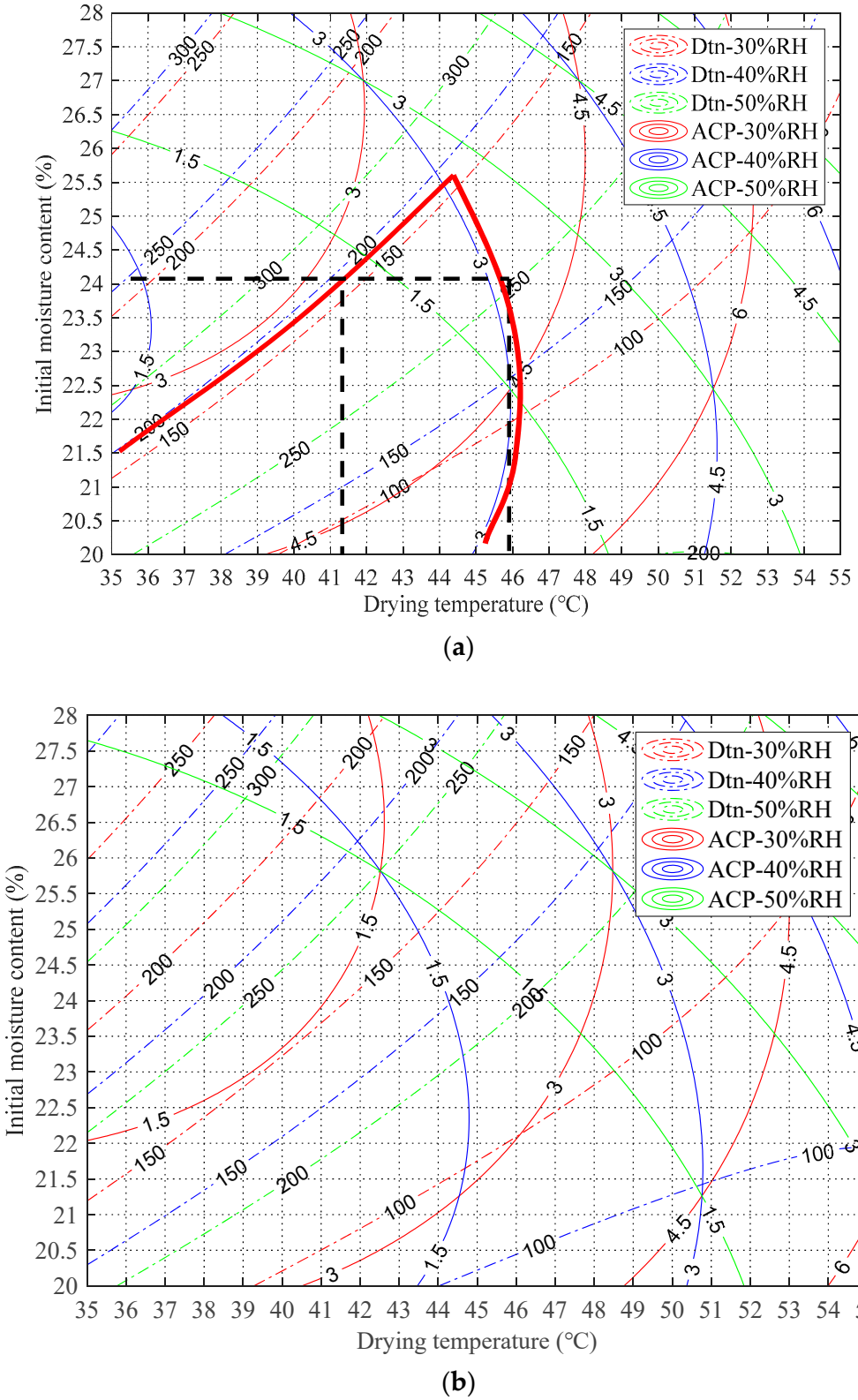

Figure 11. Process reference charts of net drying time and ACP: (**a**) TR = 2 and (**b**) TR = 3.

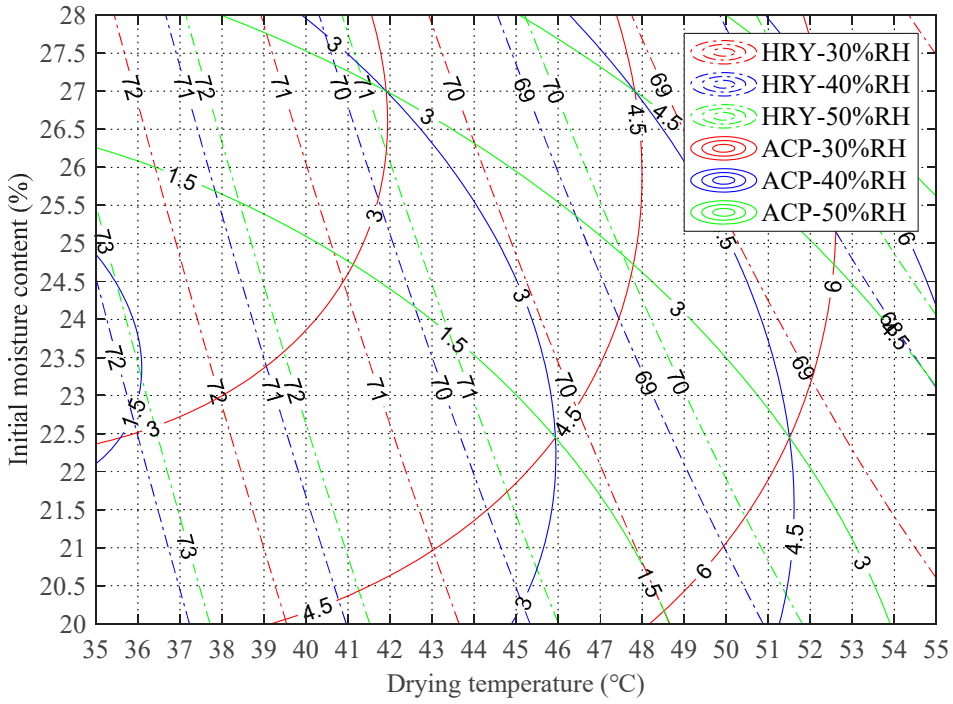

(**a**)

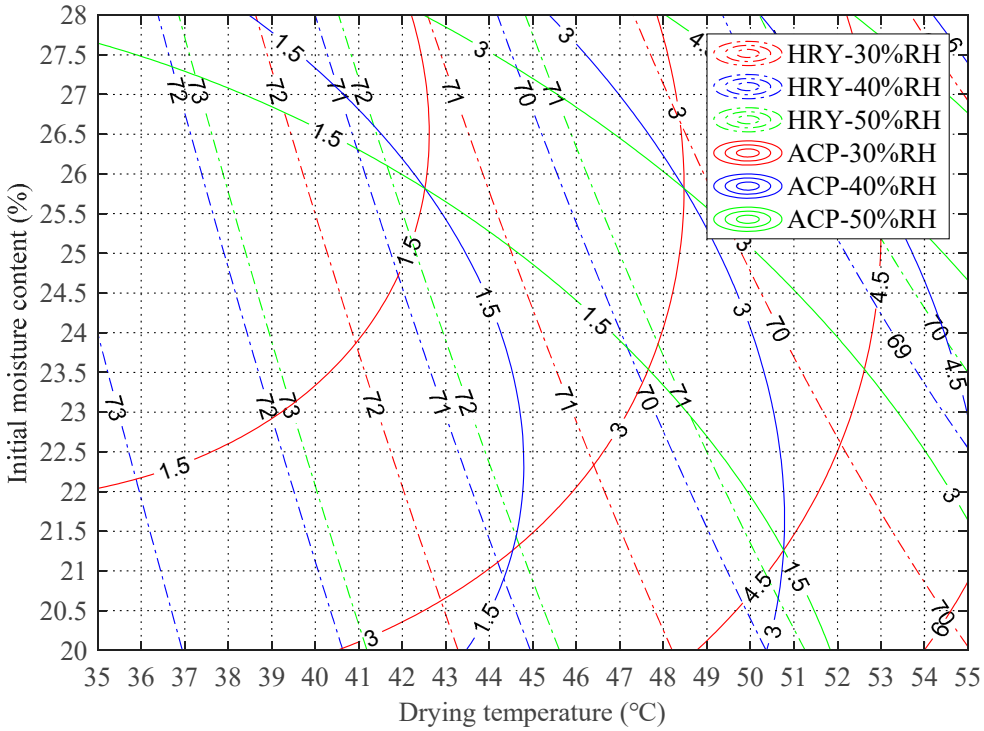

(**b**)

Figure 12. Process reference charts of ACP and HRY: (**a**) TR = 2 and (**b**) TR = 3.

4. Conclusions

The aim of this investigation was to examine the characteristics causing variations in rice quality and offer novel insights for regulating and controlling rice drying operations. A response regression model for multi-factor rice drying was established using response surface methodology (RSM) with a central composite design (CCD). The findings indicated

that all responses' quadratic polynomial models were statistically significant. In addition, it was observed that all the linear terms had significant effects on the response variables except for air velocity, which showed no significant effect on the HRY. When $p < 0.05$, T*MC significantly affected the net drying time, total drying time, and ACP; T*TR significantly affected the total drying time; RH*TR significantly affected the net drying time and ACP; and RH*MC significantly affected the ACP. Based on the RSM regression model, process reference charts were developed to guide process parameter selection and prediction. These charts can provide a high-quality control scheme within a certain range, offer valuable references for actual drying operations, and are expected to be integrated with intelligent control systems in the future. The techniques employed in constructing these charts are not restricted to the grain drying scenarios presented in this paper but can be extended to various industrial situations that necessitate parametric adjustments for controlling specific metrics. The testing methodology and model/chart construction techniques proposed in this paper hold significant reference value for the advancement of industrial control.

Author Contributions: Conceptualization, Y.J. and Z.Z.; methodology, Y.J.; software, J.Y.; validation, Z.Z. and Y.J.; formal analysis, H.X.; investigation, H.X.; resources, Y.J.; data curation, H.X.; writing—original draft preparation, Y.J.; writing—review and editing, Z.Z.; project administration, Y.J.; funding acquisition, Y.J. All authors have read and agreed to the published version of the manuscript.

Funding: This research was funded by the Academy of National Food and Strategic Reserves Administration, grant number JY2303. The APC was funded by JY2303.

Data Availability Statement: The data presented in this paper are available from the corresponding author upon request.

Acknowledgments: We express our gratitude to the reviewers for their invaluable feedback and comments on this article.

Conflicts of Interest: The authors declare no conflict of interest.

References

1. Tohidi, M.; Sadeghi, M.; Torki-Harchegani, M. Energy and quality aspects for fixed deep bed drying of paddy. *Renew. Sustain. Energy Rev.* **2017**, *70*, 519–528. [CrossRef]
2. Tong, C.; Chen, Y.; Tang, F.; Xu, F.; Huang, Y.; Chen, H.; Bao, J. Genetic diversity of amylose content and RVA pasting parameters in 20 rice accessions grown in Hainan, China. *Food Chem.* **2014**, *161*, 239–245. [CrossRef] [PubMed]
3. Reddy, K.R.N.; Reddy, C.S.; Abbas, H.K.; Abel, C.A.; Muralidharan, K. Mycotoxigenic fungi, mycotoxins, and management of rice grains. *Toxin Rev.* **2008**, *27*, 287–317. [CrossRef]
4. Oktay, H.; Ahmet, C.; Kamil, K. A liquid diffusion model for thin-layer drying of rough rice. *Eur. Food Res. Technol.* **2008**, *226*, 787–793. [CrossRef]
5. Ling, F.; Sun, T. Study on the drying characteristics of rice by microwave and hot air drying. *J. Eng.* **2021**, *4*, 201–208. [CrossRef]
6. Luthra, K.; Sadaka, S.S. Challenges and opportunities associated with drying rough rice in fluidized bed dryers: A review. *Trans. ASABE* **2020**, *63*, 583–595. [CrossRef]
7. Zhang, Q.; Yang, W.; Sun, Z. Mechanical properties of sound and fissured rice kernels and their implications for rice breakage. *J. Food Eng.* **2005**, *68*, 65–72. [CrossRef]
8. Iguaz, A.; Rodríguez, M.; Vírseda, P. Influence of handling and processing of rough rice on fissures and head rice yields. *J. Food Eng.* **2006**, *77*, 803–809. [CrossRef]
9. Hwang, S.S.; Cheng, Y.C.; Chang, C.; Lur, H.S.; Lin, T.T. Magnetic resonance imaging and analyses of tempering processes in rice kernels. *J. Cereal Sci.* **2009**, *50*, 36–42. [CrossRef]
10. Aquerreta, J.; Iguaz, A.; Arroqui, C.; Vírseda, P. Effect of high temperature intermittent drying and tempering on rough rice quality. *J. Food Eng.* **2007**, *80*, 611–618. [CrossRef]
11. Dong, R.; Lu, Z.; Liu, Z.; Koide, S.; Cao, W. Effect of drying and tempering on rice fissuring analysed by integrating intra-kernel moisture distribution. *J. Food Eng.* **2010**, *97*, 161–167. [CrossRef]
12. Shei, H.J.; Chen, Y.L. Computer simulation on intermittent drying of rough rice. *Dry. Technol.* **2007**, *20*, 615–636. [CrossRef]
13. Golmohammadi, M.; Rajabi-Hamane, M.; Hashemi, S.J. Optimization of Drying–Tempering Periods in a Paddy Rice Dryer. *Dry. Technol.* **2012**, *30*, 106–113. [CrossRef]
14. Zecchi, B.; Gerla, P. Breakage and mass transfer models during drying of rough rice. *Dry. Technol.* **2007**, *25*, 1405–1410. [CrossRef]
15. Nanvakenari, S.; Movagharnejad, K.; Latifi, A. Evaluating the fluidized-bed drying of rice using response surface methodology and artificial neural network. *LWT* **2021**, *147*, 111589. [CrossRef]

16. Huang, X.; Li, W.; Wang, Y.; Wan, F. Drying characteristics and quality of Stevia rebaudiana leaves by far-infrared radiation. *LWT* **2021**, *140*, 110638. [CrossRef]
17. Jin, Y.; Wong, K.W.; Wu, Z.; Qi, D.; Wang, R.; Han, F.; Wu, W. Relationship between accumulated temperature and quality of paddy. *Int. J. Food Prop.* **2019**, *22*, 19–33. [CrossRef]
18. Li, Y.B.; Cao, C.W.; Yu, Q.L.; Zhong, Q.X. Study on rough rice fissuring during intermittent drying. *Dry. Technol.* **1998**, *17*, 1779–1793. [CrossRef]
19. Sharma, A.D.; Kunze, O.R. Post-Drying Fissure Developments in Rough Rice. *Trans. ASAE* **1982**, *25*, 465–468. [CrossRef]
20. Dibagar, N.; Amiri Chayjan, R. Rough rice convective drying enhancement by intervention of airborne ultrasound—A response surface strategy for experimental design and optimization. *Dry. Technol.* **2019**, *37*, 1097–1112. [CrossRef]
21. Soltani, A.; Azzouz, S.; Romdhana, H.; Goujot, D.; El Cafsi, M.A. Multi-response optimization of drying process parameters for Laurus Nobilis. *J. Appl. Res. Med. Aromat. Plants* **2021**, *22*, 100302. [CrossRef]
22. Kumar, D.; Prasad, S.; Murthy, G.S. Optimization of microwave-assisted hot air drying conditions of okra using response surface methodology. *J. Food Sci. Technol.* **2014**, *51*, 221–232. [CrossRef] [PubMed]
23. Li, Y.; Liu, Z.; Zhao, H.; Xu, Y.; Cui, F. Statistical optimization of xylanase production from new isolated Penicillium oxalicum ZH-30 in submerged fermentation. *Biochem. Eng. J.* **2007**, *34*, 82–86. [CrossRef]
24. Šumić, Z.; Vakula, A.; Tepić, A.; Čakarević, J.; Vitas, J.; Pavlić, B. Modeling and optimization of red currants vacuum drying process by response surface methodology (RSM). *Food Chem.* **2016**, *203*, 465–475. [CrossRef]
25. Onwude, D.I.; Hashim, N.; Chen, G. Recent advances of novel thermal combined hot air drying of agricultural crops. *Trends Food Sci. Technol.* **2016**, *57*, 132–145. [CrossRef]
26. Sagar, V.R.; Suresh Kumar, P. Recent advances in drying and dehydration of fruits and vegetables: A review. *J. Food Sci. Technol.* **2010**, *47*, 15–26. [CrossRef] [PubMed]
27. Vimercati, W.C.; da Silva Araújo, C.; Macedo, L.L.; Maradini Filho, A.M.; Saraiva, S.H.; Teixeira, L.J.Q. Influence of drying temperature on drying kinetics, energy consumption, bioactive compounds and cooking quality of pasta enriched with spinach. *J. Food Process Eng.* **2020**, *43*, e13571. [CrossRef]
28. Bertotto, M.M.; Gastón, A.; Sánchez Sarmiento, G.; Gove, B. Effect of drying conditions on the quality of IRGA 424 rice. *J. Sci. Food Agric.* **2019**, *99*, 1651–1659. [CrossRef]
29. Candioti, L.V.; De Zan, M.M.; Cámara, M.S.; Goicoechea, H.C. Experimental design and multiple response optimization. Using the desirability function in analytical methods development. *Talanta* **2014**, *124*, 123–138. [CrossRef]
30. Müller, A.; Nunes, M.T.; Maldaner, V.; Coradi, P.C.; Moraes, R.S.d.; Martens, S.; Leal, A.F.; Pereira, V.F.; Marin, C.K. Rice Drying, Storage and Processing: Effects of Post-Harvest Operations on Grain Quality. *Rice Sci.* **2022**, *29*, 16–30. [CrossRef]

Disclaimer/Publisher's Note: The statements, opinions and data contained in all publications are solely those of the individual author(s) and contributor(s) and not of MDPI and/or the editor(s). MDPI and/or the editor(s) disclaim responsibility for any injury to people or property resulting from any ideas, methods, instructions or products referred to in the content.